Inorg. Chem. **2007**, *46*, 4298–4307

Oligonuclear Copper Complexes of a Bioinspired Pyrazolate-Bridging Ligand: Synthesis, Structures, and Equilibria in Solution

Angelina Prokofieva,[‡] Alexander I. Prikhod'ko,[‡] Eva Anna Enyedy,[†] Etelka Farkas,[†] Walter Maringgele,[‡] Serhiy Demeshko,[‡] Sebastian Dechert,[‡] and Franc Meyer*[,‡]

Institut für Anorganische Chemie, Georg-August-Universität, Tammannstrasse 4, D-37077 Göttingen, Germany, and Department of Inorganic and Analytical Chemistry, Faculty of Science, University of Debrecen, H-4010 Debrecen, Hungary

Received December 19, 2006

The synthesis of a new bioinspired dinucleating ligand scaffold based on a bridging pyrazolate with appended bis[2-(1-methylimidazolyl)methyl]aminomethyl chelate arms is reported. This ligand forms very stable copper complexes, and a series of different species is present in solution depending on the pH. Interconversions between these solution species are tracked and characterized spectroscopically, and X-ray crystallographic structures of three distinct complexes that correspond to the species present in solution from acidic to basic pH have been determined. Overall, this provides a comprehensive picture of the copper coordination chemistry of the new ligand system. Alterations in the protonation state are accompanied by changes in nuclearity and pyrazolate binding, which cause pronounced changes in color and magnetic properties. Antiferromagnetic coupling between the copper(II) ions is switched on or off depending on the pyrazole binding mode.

Introduction

Preorganized dinuclear transition metal complexes have received a lot of attention over the past several years, mainly because of increasing interest in cooperative effects between individual metal centers.[1] Scaffolds to support and control a bimetallic arrangement may be provided by compartmental binucleating ligand matrices that host two metal ions in suitable proximity.[2] Major stimulus for this development comes from the unique reactivity patterns of various bimetallic enzyme active sites, which often feature two cooperating metal ions at distances between 2.8 and 4.5 Å embedded in the protein. Hence the design of synthetic ligands that provide a biomimetic donor environment has evolved as a guide line in modern coordination chemistry. Pyrazolate-based ligands with chelating side arms in the 3- and 5-positions of the heterocycle have been developed as valuable scaffolds in this regard: the anionic pyrazolate has a high tendency to span two metal ions, and the individual coordination spheres, as well as the metal−metal separations, can be tuned by appropriate alterations of the appended chelate substituents.[3−7] Type **B** bimetallic complexes with pyrazolate-bridging ligands can be described as two tripodal tetradentate $\{N_4\}$ subunits **A** coupled by the central heterocyclic moiety (Chart 1). The preferred metal−metal separations range from 3.4 to 4.5 Å depending on the length of the outer side arms.[3,5,6]

Mononuclear complexes of tripodal tetradentate ligands **A** have proven to be highly successful for the emulation of

* To whom correspondence should be addressed. E-mail: franc.meyer@chemie.uni-goettingen.de.
‡ Georg-August-Universität Göttingen.
† University of Debrecen.

(1) (a) Steinhagen, H.; Helmchen, G. *Angew. Chem.* **1996**, *108*, 2489−2492; *Angew. Chem., Int. Ed. Engl.* **1996**, *35*, 2339−2342. (b) Fenton, D. E.; Okawa, H. *Chem. Ber./Recl.* **1997**, *130*, 433−442. (c) Van den Beuken, E. K.; Feringa, B. L. *Tetrahedron* **1998**, *54*, 12985−13011. (d) Bosnich, B. *Inorg. Chem.* **1999**, *38*, 2554−2562. (e) Belle, C.; Pierre, J.-L. *Eur. J. Inorg. Chem.* **2003**, 4137−4146.

(2) (a) Fenton, D. E.; Casellato, U.; Vigato, P. A.; Vidali, M. *Inorg. Chim. Acta* **1982**, *62*, 57−66. (b) Gavrilova, A. L.; Bosnich, B. *Chem. Rev.* **2004**, *104*, 349−383.

(3) Klingele, J.; Dechert, S.; Meyer, F. *Coord. Chem. Rev.* Submitted for publication.

(4) Schenck, T. G.; Downes, J. M.; Milne, C. R. C.; Mackenzie, P. B.; Boucher, H.; Whelan, J.; Bosnich, B. *Inorg. Chem.* **1985**, *24*, 2334−2337.

(5) (a) Meyer, F.; Beyreuther, S.; Heinze, K.; Zsolnai, L. *Chem. Ber./Recl.* **1997**, *130*, 605−613. (b) Meyer, F.; Heinze, K.; Nuber, B.; Zsolnai, L. *J. Chem. Soc., Dalton Trans.* **1998**, 207−213. (c) Konrad, M.; Meyer, F.; Heinze, K.; Zsolnai, L. *J. Chem. Soc., Dalton Trans.* **1998**, 199−205. (d) Buchler, S.; Meyer, F.; Jacobi, A.; Kircher, P.; Zsolnai, L. *Z. Naturforsch.* **1999**, *54b*, 1295−1306. (e) Konrad, M.; Wuthe, S.; Meyer, F.; Kaifer, E. *Eur. J. Inorg. Chem.* **2001**, 2233−2240. (f) Buchler, S.; Meyer, F.; Kaifer, E.; Pritzkow, H. *Inorg. Chim. Acta* **2002**, *337*, 371−386. (g) Röder, J. C.; Meyer, F.; Kaifer, E.; Pritzkow, H. *Eur. J. Inorg. Chem.* **2004**, 1646−1660. (h) Ackermann, J.; Meyer, F.; Pritzkow, H. *Inorg. Chim. Acta* **2004**, *357*, 3703−3711.

(6) Siegfried, L.; Kaden, T. A.; Meyer, F.; Kircher, P.; Pritzkow, H. *J. Chem. Soc., Dalton Trans.* **2001**, 2310−2315.

10.1021/ic062434m CCC: $37.00
Published on Web 04/11/2007

Chart 1

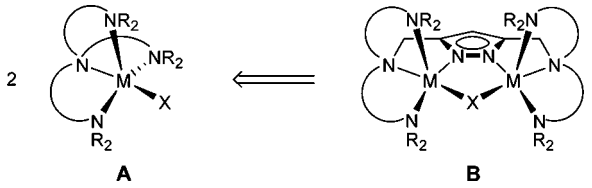

the properties and reactivities of monometallic N-ligated metallobiosites.[8] This is particularly true in biomimetic copper/dioxygen chemistry where manifold variations of motif **A** have been employed, most prominently ligands of the tris(pyridylmethyl)amine type.[9,10] For their bimetallic analogues **B**, a similarly rich bioinorganic chemistry is just emerging and offers great prospects because of the potential of the highly preorganized proximate metal ions to work in concert during substrate transformations.[11,12,13] Pyrazolate-bridging compartmental ligands used until now feature, inter alia, aliphatic side arms with secondary or tertiary amine donors or substituents with pyridyl groups.[3] With the aim of further advancing the emulation of biological donor environments in type **B** scaffolds, we have now prepared a new pyrazolate-based ligand L that has binding compartments composed of imidazolyl groups. To use dinuclear copper

Scheme 1. Preparation of the New Ligand L Used in This Work

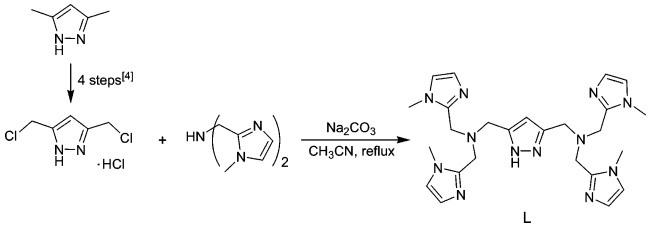

complexes of this new ligand in bioinspired reactions, profound knowledge about their structural characteristics and their behavior in solution is a prerequisite. Here we report the complexation equilibria and the stability of Cu^{2+} complexes of L in solution, as well as crystallographic and magnetic studies of the different complexes in the solid state.

Results and Discussion

Ligand Synthesis and Species Distribution with Copper(II). Ligand L was synthesized in good yield following a strategy developed previously.[3,5h] The final step is the coupling of 3,5-bis(chloromethyl)pyrazole hydrochloride (prepared in 4 steps from 3,5-dimethylpyrazole)[4] with bis-[2-(1-methylimidazolyl)methyl]amine[14] (Scheme 1). L was obtained as slightly yellowish solid and was characterized by NMR spectroscopy, mass spectrometry and microanalysis.

After deprotonation, L should be capable of providing two binding pockets, each reminiscent of the tripodal tetradentate tris(2-(1-imidazolyl)methyl)amine ligand that is known to form trigonal bipyramidal copper(II) complexes **C**.[15] In this regard, the anticipated dicopper complexes **D** can be viewed as a pyrazolate-bridging dinucleating version of two coupled type **C** subunits. Potentiometric titrations were carried out to determine the pK_a values of the new ligand and to probe its copper(II) coordination chemistry.

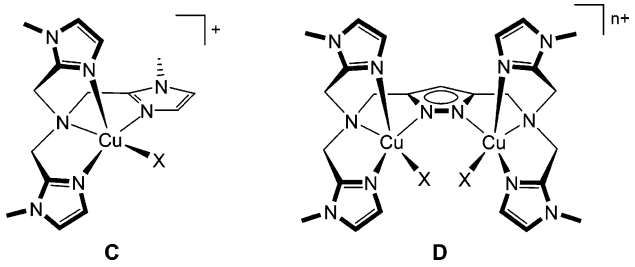

Ligand Protonation Constants. Titrations were performed starting at acidic pH using a potassium hydroxide titrant. From the titration curves, the deprotonation steps can be derived (Figure S2 and Table 1). The processes occurring in the measurable pH range between approximately pH 4 and 9 belong to the dissociation of one proton per protonated imidazole moiety. The difference between the sequential dissociation constants is higher (~0.8 log units) than expected for statistical reasons, which suggests some interaction (most probably through space) between the individual

(7) (a) Kamiusuki, T.; Okawa, H.; Matsumoto, N.; Kida, S. *J. Chem. Soc., Dalton Trans.* **1990**, 195−198. (b) Mernari, B.; Abraham, F.; Lagrenee, M.; Drillon, M.; Legoli, P. *J. Chem. Soc., Dalton Trans.* **1993**, 1707−1711. (c) Weller, H.; Siegfried, L.; Neuburger, M.; Zehnder, M.; Kaden, T. A. *Helv. Chim. Acta* **1997**, *80*, 2315−2328. (d) Kaden, T. A. *Coord. Chem. Rev.* **1999**, *190−192*, 371−389. (e) Tanaka, S.; Dubs, C.; Inagaki, A.; Akita, M. *Organometallics* **2005**, *24*, 163−184. (f) Miranda, C.; Escarti, F.; Lamarque, L.; Garcia-Espana, E.; Navarro, P.; Latorre, J.; Lloret, F.; Jimenez, H. R.; Yunta, M. J. R. *Eur. J. Inorg. Chem.* **2005**, 189−208. (g) Zinn, P. J.; Powell, D. R.; Day, V. W.; Hendrich, M. P.; Sorrell, T. N.; Borovik, A. S. *Inorg. Chem.* **2006**, *45*, 3484−3486.

(8) Berreau, L. M. *Eur. J. Inorg. Chem.* **2006**, 273−283.

(9) (a) Schindler, S. *Eur. J. Inorg. Chem.* **2000**, 2311−2326. (b) Würtele, C.; Gaoutchenova, E.; Harms, K.; Holthausen, M. C.; Sundermeyer, J.; Schindler, S. *Angew. Chem.* **2006**, *118*, 3951−3954; *Angew. Chem., Int. Ed.* **2006**, *45*, 3867−3869.

(10) (a) Jacobson, R. J.; Tyeklar, Z.; Farooq, A.; Karlin, K. D.; Liu, S.; Zubieta J. *J. Am. Chem. Soc.* **1988**, *110*, 3690−3692. (b) Wei, N.; Murthy, N. N.; Tyeklar, Z.; Karlin, K. D. *Inorg. Chem.* **1994**, *33*, 1177−1183. (b) Schatz, M.; Becker, M.; Thaler, F.; Hampel, F.; Schindler, S.; Jacobson, R. R.; Tyeklar, Z.; Murthy, N. N.; Ghosh, P.; Chen, Q.; Zubieta, J.; Karlin, K. *Inorg. Chem.* **2001**, *40*, 2312−2322. (c) Uozumi, K.; Hayashi, Y.; Suzuki, M.; Uehara, A. *Chem. Lett.* **1993**, 963−966. (d) Komiyama, K.; Furutachi, H.; Nagatomo, S.; Hashimoto, A.; Hayashi, H.; Fujinami, S.; Suzuki, M.; Kitagawa, T. *Bull. Chem. Soc. Jpn.* **2004**, *77*, 59−72.

(11) (a) Meyer, F.; Rutsch, P. *Chem. Commun.* **1998**, 1037−1038. (b) Meyer, F.; Pritzkow, H. *Chem. Commun.* **1998**, 1555−1556. (c) Meyer, F.; Kaifer, E.; Kircher, P.; Heinze, K.; Pritzkow, H. *Chem.−Eur. J.* **1999**, *5*, 1617−1630. (d) Meyer, F.; Hyla-Kryspin, I.; Kaifer, E.; Kircher, P. *Eur. J. Inorg. Chem.* **2000**, 771−781. (e) Kryatov, S. V.; Rybak-Akimova, E. V.; Meyer, F.; Pritzkow, H. *Eur. J. Inorg. Chem.* **2003**, 1581−1590. (f) Bauer-Siebenlist, B.; Meyer, F.; Farkas, E.; Vidovic, D.; Seijo, J. A. C.; Herbst-Irmer, R.; Pritzkow, H. *Inorg. Chem.* **2004**, *43*, 4189−4202. (g) Bauer-Siebenlist, B.; Meyer, F.; Farkas, E.; Vidovic, D.; Dechert, S. *Chem.−Eur. J.* **2005**, *11*, 4349−4360. (h) Bauer-Siebenlist, B.; Dechert, S.; Meyer, F. *Chem.−Eur. J.* **2005**, *11*, 5343−5352.

(12) (a) Meyer, F.; Pritzkow, H. *Angew. Chem.* **2000**, *112*, 2199−2202; *Angew. Chem., Int. Ed.* **2000**, *39*, 2112−2115. (b) Ackermann, J.; Meyer, F.; Kaifer, E.; Pritzkow, H. *Chem.−Eur. J.* **2002**, *8*, 247−258. (c) Ackermann, J.; Buchler, S.; Meyer, F. *C. R. Chimie* **2007**, in press.

(13) (a) Vichard, C.; Kaden, T. A. *Inorg. Chim. Acta* **2002**, *337*, 173−180. (b) Vichard, C.; Kaden, T. A. *Inorg. Chim. Acta* **2004**, *357*, 2285−2293.

(14) Oberhausen, K. J.; Richardson, J. F.; Buchanan, R. M.; Pierce, W. *Polyhedron* **1989**, *8*, 659−668.

(15) Oberhausen, K. J.; O'Brien, R. J.; Richardson, J. F.; Buchanan, R. M. *Inorg. Chim. Acta* **1990**, *173*, 145−154.

Table 1. Overall Protonation Constants (log β) and Sequential Dissociation Constants (pK_a) of the Ligand L at 25 °C with $I = 0.2$ M (KCl)[a]

	$[LH_4]^{4+}$	$[LH_3]^{3+}$	$[LH_2]^{2+}$	$[LH]^{+}$
log β	26.06(1)	20.78(1)	14.71(2)	7.77(1)
pK_a	5.28	6.07	6.94	7.77

[a] Standard deviations are given in parenthesis

Table 2. Overall Stability Constants (log β) and Some Dissociation Constants (pK_a) for the Complexes Formed with Cu^{2+} at 25 °C with $I = 0.2$ M (KCl)[a]

	$[CuLH_2]^{4+}$	$[Cu_2L]^{4+}$	$[Cu_2LH_{-1}]^{3+}$	$[Cu_2LH_{-2}]^{2+}$
log β	26.36(4)	23.56(3)	17.79(8)	9.85(9)
pK_a		5.77	7.94	

[a] Standard deviations are given in parenthesis

protonation sites. According to the experimental results, protonation of the pyrazole to give a putative $[LH_5]^{5+}$ occurs only below pH 2, and the stability constant was not determined for this process.

Species Distribution of Copper Complexes. Titrations of L in the presence of various equivalents of Cu^{2+} were analyzed in batch calculations in which all titration curves are fitted at the same time with one model (Figure S3 and Table 2). Evaluation of the titration curves shows that the Cu^{2+}-binding capabilities of L are high. Although free Cu^{2+} ions and the mononuclear species $[CuLH_2]^{4+}$ are observable up to pH ~4, the dinuclear species $[Cu_2L]$ is already formed at around pH 2 and becomes almost the sole species around pH 4 (Figure 1). This dinuclear complex present at rather acidic conditions presumably has a non-deprotonated (i.e., nonbridging) pyrazole unit. $[Cu_2LH_{-1}]^{3+}$ starts to form above pH 4 and exists in solution up to pH 10. It is the dominant species at pH 7 and most likely is a pyrazolato-bridged complex, where the heterocycle is deprotonated. A further deprotonation step leads to dinuclear $[Cu_2LH_{-2}]^{2+}$ which is the major species under more basic conditions. The calculated pK_a value of 7.94 for $[Cu_2LH_{-1}]^{3+}$ represents the acidity of a metal-bound water to give $[Cu_2LH_{-2}]^{2+}$, that is, the latter species is better described as $[Cu_2LH_{-1}(OH)]^{2+}$. The Zn^{2+} complex of tris(2-(1-imidazolyl)methyl)amine shows pK_a = 8.72 for a metal-bound water,[16] and the value for the corresponding mononuclear Cu^{2+} system (**C** with X = H_2O) should be even higher. Hence there is a clear increase in water acidity because of the bimetallic arrangement in $[Cu_2LH_{-1}]^{3+}$, and its relatively low pK_a value suggests a bridging position of the water or incorporation of the resulting hydroxide in a strongly hydrogen-bonded O_2H_3 moiety within the bimetallic pocket. However, acidification of the Cu-bound water is less pronounced than in related pyrazolate-bridged systems with aliphatic N-donor side arms attached to the heterocycle.[6]

UV−vis spectra were recorded for aqueous solutions containing L and 2 equiv of $Cu(NO_3)_2$ at pH 4.6, 6.5, and 9.4 to further characterize the species $[Cu_2L]^{4+}$, $[Cu_2LH_{-1}]^{3+}$, and $[Cu_2LH_{-2}]^{2+}$ present under those conditions (Figure 2). The spectral features of the $[Cu_2LH_{-2}]^{2+}$ species at pH 9.4

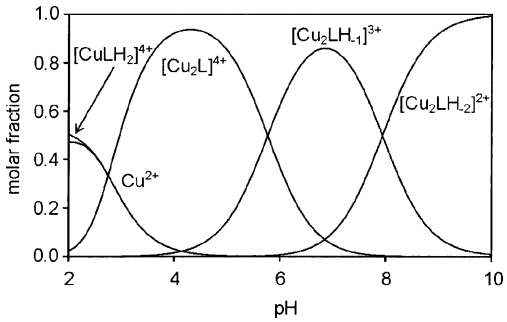

Figure 1. Concentration distribution of the species formed between L and Cu^{2+} at a 1:2 ligand to metal ratio. $c_L = 1.5 \times 10^{-3}$ M.

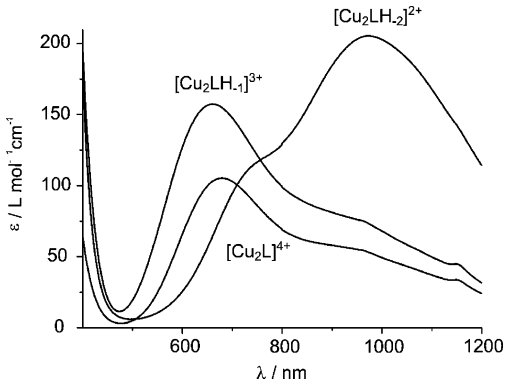

Figure 2. UV−vis spectra of L with 2 equiv of $Cu(NO_3)_2$ in H_2O at pH 4.6 (a), 6.5 (b), and 9.4 (c). Weak features at ~1050 nm are artifacts caused by the spectrometer.

Table 3. UV−vis Data of L with 2 equiv of $Cu(NO_3)_2$ in Aqueous Solution at Different pHs and of Individual Complexes **1a**, **2**, and **3** in MeOH/MeCN (5:2) and in the Solid State (Diffuse Reflectance)[a]

species	H_2O	complex	MeOH/MeCN (5:2)	diffuse reflectance
$[Cu_2LH_{-2}]^{2+}$	741 (110), 972 (204)	**1a**	730 (135), 962 (269)	952
$[Cu_2LH_{-1}]^{3+}$	663 (157)	**2**	689 (281), 923 (272)	705, 918
$[Cu_2L]^{4+}$	676 (105)	**3**	677 (96)	689

[a] λ [nm] (ϵ [L mol^{-1} cm^{-1}]).

indicate a trigonal bipyramidal coordination geometry for both copper ions (λ_{max} = 972 nm), while the species $[Cu_2L]^{4+}$ and $[Cu_2LH_{-1}]^{3+}$ which are present at pH 4.6 and 6.5, respectively, have absorption maxima typical for copper in a square pyramidal environment ($\lambda_{max} \approx 670$ nm, Table 3).[17]

Structural Characterization of Complexes. Three distinctly different copper(II) complexes **1**−**3** of the pyrazolate-based ligand L could be isolated from solutions at appropriate pH, reflecting the protonation state of the three different species $[Cu_2L]^{4+}$, $[Cu_2LH_{-1}]^{3+}$, and $[Cu_2LH_{-2}]^{2+}$ (Scheme 2). Single crystals of **1a**, **1b**, **2**, and **3** were obtained, and their molecular structures were elucidated by X-ray crystallography.

The addition of 2 equiv of $Cu(NO_3)_2$ to a MeOH/H_2O solution containing L and 1 equiv of base (KO*t*Bu) produced a green-blue reaction mixture that was subjected to ion-exchange chromatography using a SP-Sephadex C25 column, giving a blue solution. The adjustment of the pH of this

(16) Chiu, Y.-H.; Canary, J. W. *Inorg. Chem.* **2003**, *42*, 5107−5116.

(17) Lever A. B. P. *Inorganic Electronic Spectroscopy*; Elsevier: Amsterdam, The Netherlands, 1984.

Scheme 2. Schematic Representation of Copper Complexes of Ligand L Isolated under Different pH Conditions

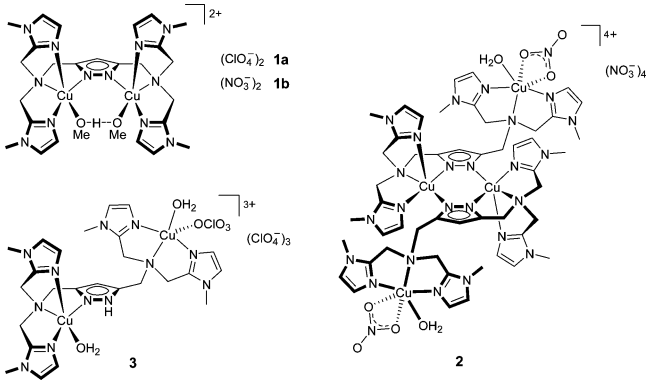

solution to 9 and the addition of $NaClO_4$ precipitated a green powder that was crystallized from MeCN/MeOH/Et_2O to yield complex **1a**. The corresponding nitrate salt **1b** can be prepared directly via the addition of 2 equiv of base (KO*t*Bu) and 2 equiv of $Cu(NO_3)_2$ to a solution of L, followed by crystallization from MeCN/MeOH/Et_2O. Molecular structures of the cations of **1a** and **1b** are very similar, and the molecular structure of the former is shown in Figure 3, together with selected atomic distances and bond angles.

The two copper ions in **1a** reside within the adjacent $\{N_4\}$ ligand compartments of LH_{-1} and are bridged by the pyrazolate, as anticipated. Both metal ions are five-coordinate with slightly distorted trigonal-bipyramidal geometry (τ = 0.88),[18] in accordance with the solution UV−vis data for $[Cu_2LH_{-2}]^{2+}$. The pyrazolate-N and the two imidazole-N units constitute the equatorial plains, while the axial positions are occupied by the tertiary N atoms of the ligand backbone and by the O atoms of a MeOH···OMe moiety located within the bimetallic pocket. The O···O distance of 2.41 Å is quite short and indicates the presence of a very strong hydrogen bond.[19] This motif closely resembles the situation observed for some Ni^{2+}, Cu^{2+}, and Zn^{2+} complexes of related pyrazole-derived ligands with pyridyl or aliphatic N-donor chelate substituents, where it was shown that the accessible range of metal−metal separations is determined by the length of the side arms appended to the pyrazole.[5,6,11] The rather short side arms of L give five-membered chelate rings and thus enforce rather large Cu···Cu distances that prevent a small hydroxide or methoxide from spanning the two metal ions. The incorporation of an additional MeOH solvent molecule then furnishes the MeOH···OMe bridging unit observed for **1a** (d(Cu···Cu) = 4.340 Å). Such units have previously been shown to undergo rapid ligand exchange with, for example, water.[11e] Therefore the species $[Cu_2LH_{-2}]^{2+}$ that is present in aqueous solution at high pH most certainly contains an analogous HOH···OH bridge and should thus be best formulated as $[Cu_2LH_{-1}(O_2H_3)]^{2+}$. It should be noted that a $Zn(O_2H_3)Zn$ core has been discussed as the active species of some dizinc metallohydrolases.[11a,f,g,20,21]

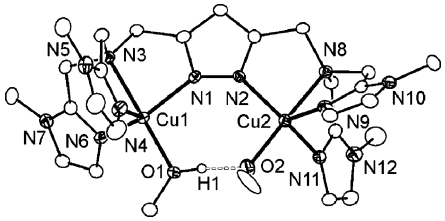

Figure 3. ORTEP plot (30% probability thermal ellipsoids) of the cation of **1a**. Disorder and hydrogen atoms except H1 are not shown for clarity. Selected atom distances (Å) and angles (deg): Cu1−O1 = 1.915(2), Cu1−N1 = 2.030(3), Cu1−N3 = 2.129(3), Cu1−N4 = 2.080(3), Cu1−N6 = 2.013(3), Cu2−O2 = 1.929(3), Cu2−N2 = 2.007(3), Cu2−N8 = 2.111(3), Cu2−N9 = 2.085(3), Cu2−N11 = 2.087(3), Cu1···Cu2 = 4.3405(6), O1···O2 = 2.407(4); O1−Cu1−N1 = 96.4(1), O1−Cu1−N3 = 177.3(1), O1−Cu1−N4 = 101.5(1), O1−Cu1−N6 = 96.4(1), N1−Cu1−N3 = 80.8(1), N1−Cu1−N4 = 109.1(1), N1−Cu1−N6 = 124.2(1), N3−Cu1−N4 = 81.0(1), N3−Cu1−N6 = 81.4(1), N4−Cu1−N6 = 119.47(1), O2−Cu2−N2 = 99.8(1), O2−Cu2−N8 = 174.8(1), O2−Cu2−N9 = 104.2(1), O2−Cu2−N11 = 96.9(1), N2−Cu2−N8 = 80.3(1), N2−Cu2−N9 = 118.5(1), N2−Cu2−N11 = 121.4(1), N8−Cu2−N9 = 80.1(1), N8−Cu2−N11 = 78.8(1), N9−Cu2−N11 = 110.7(1), O1−H1···O2 = 173(5).

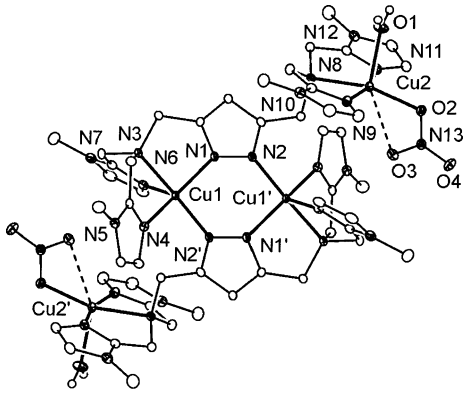

Figure 4. ORTEP plot (30% probability thermal ellipsoids) of the cation of **2**. Hydrogen atoms except H1A/B are not shown for clarity. Selected atom distances (Å) and angles (deg): Cu1−N1 = 2.020(2), Cu1−N2′ = 1.949(2), Cu1−N3 = 2.117(2), Cu1−N4 = 2.106(2), Cu1−N6 = 2.074(2), Cu2−O1 = 2.222(2), Cu2−O2 = 1.996(2), Cu2−O3 = 2.651(2), Cu2−N8 = 2.111(2), Cu2−N9 = 1.941(2), Cu2−N11 = 1.952(2), Cu1···Cu1′ = 3.8674(6); N1−Cu1−N2′ = 100.72(8), N1−Cu1−N3 = 79.93(8), N1−Cu1−N4 = 119.64(8), N1−Cu1−N6 = 119.71(8), N2′−Cu1−N3 = 174.15(8), N2′−Cu1−N4 = 95.70(8), N2′−Cu1−N6 = 103.90(8), N3−Cu1−N4 = 79.04(8), N3−Cu1−N6 = 80.59(8), N4−Cu1−N6 = 111.51(8), O1−Cu2−O2 = 100.31(8), O1−Cu2−N8 = 96.23(8), O1−Cu2−N9 = 92.41(9), O1−Cu2−N11 = 88.62(8), O2−Cu2−N8 = 163.40(7), O2−Cu2−N9 = 95.77(8), O2−Cu2−N11 = 99.77(8), N8−Cu2−N9 = 82.03(8), N8−Cu2−N11 = 81.97(8), N9−Cu2−N11 = 163.98(9). Symmetry transformation used to generate equivalent atoms (′): $1-x$, $1-y$, $1-z$.

A tetranuclear copper complex **2** could be isolated directly from the blue aqueous solution obtained after ion-exchange chromatography (see above). The protonation state of **2** relates it to the species $[Cu_2LH_{-1}]^{3+}$ that predominates in solution around neutral pH, that is, the pyrazolate is deprotonated but no additional hydroxide is present. The molecular structure of the cation of **2** is shown in Figure 4.

Unexpectedly, X-ray crystallography of **2** reveals a dimeric arrangement of two $\{LCu_2\}$ subunits that features a central bis(pyrazolato) bridged dicopper(II) core. These two copper(II) ions have an almost perfect trigonal bipyramidal $\{N_5\}$ coordination environment (τ = 0.91), where one of the apical

(18) Addison, A. W.; Rao, T. N.; Reedijk, J.; Van Rijn, J.; Verschoor, G. C. *J. Chem. Soc., Dalton. Trans.* **1982**, 1349.
(19) Emsley, J. *Chem. Soc. Rev.* **1980**, *9*, 91−124.
(20) Ruf, M.; Weis, K.; Vahrenkamp, H. *J. Am. Chem. Soc.* **1996**, *118*, 9288−9294.
(21) (a) Erhardt, S.; Jaime, E.; Weston, J. *J. Am. Chem. Soc.* **2005**, *127*, 3654−3655. (b) Jaime, E.; Weston, J. *Eur. J. Inorg. Chem.* **2006**, 793−801.

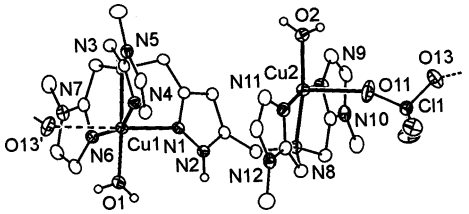

Figure 5. ORTEP plot (30% probability thermal ellipsoids) of the cation of **3**. Hydrogen atoms except H1A/B and H2A/B are not shown for clarity. Selected atom distances (Å) and angles (deg): Cu1−O1 = 1.990(3), Cu1−O13 = 2.761(4), Cu1−N1 = 2.244(4), Cu1−N3 = 2.146(3), Cu1−N4 = 1.946(4), Cu1−N6 = 1.945(4), Cu2−O2 = 1.955(3), Cu2−O11 = 2.398(4), Cu2−N8 = 2.076(3), Cu2−N9 = 1.945(4), Cu2−N11 = 1.957(4), Cu1···Cu2 = 6.7645(8); O1−Cu1−N1 = 102.1(1), O1−Cu1−N3 = 177.1(2), O1−Cu1−N4 = 98.7(2), O1−Cu1−N6 = 96.0(2), N1−Cu1−N3 = 80.7(1), N1−Cu1−N4 = 103.2(2), N1−Cu1−N6 = 92.4(2), N3−Cu1−N4 = 80.9(1), N3−Cu1−N6 = 83.4(1), N4−Cu1−N6 = 155.8(2), O2−Cu2−O11 = 86.6(2), O2−Cu2−N8 = 172.0(2), O2−Cu2−N9 = 99.6(2), O2−Cu2−N11 = 96.0(2), O11−Cu2−N8 = 101.1(2), O11−Cu2−N9 = 93.4(2), O11−Cu2−N11 = 88.8(2), N8−Cu2−N9 = 81.9(2), N8−Cu2−N11 = 82.5(2), N9−Cu2−N11 = 164.4(2). Symmetry transformation used to generate equivalent atoms (′): $1.5 - x$, $1 - y$, $-0.5 + z$.

Cu−N bonds is slightly elongated at d(Cu1−N3) = 2.117(2) Å. The remaining ligand side arms are dangling and host the other two copper ions, whose coordination sphere consist of three side arm N atoms and one water molecule. An overall square-pyramidal geometry of those outer metal ions is completed by an O-bound nitrate, but the additional weak interaction of the metal with a second O atom of the nitrate (Cu2···O3 2.651(2) Å) increases the coordination number to six and extends the coordination sphere to a strongly Jahn−Teller-distorted octahedron.

Acidification of the blue solution obtained after ion-exchange chromatography (see above) to pH ∼4 by the addition of aqueous $HClO_4$ yielded crystalline material of complex **3** that relates to the solution species $[Cu_2L]^{4+}$. As was already concluded from the titration data, **3** has a non-deprotonated pyrazole. The molecular structure of its cation is shown in Figure 5, together with selected atom distances and bond angles.

Compound **3** can be described as one-half of **2**, since protonation of the pyrazolate splits the central bis(pyrazolato)dicopper core and leaves only one of the copper ions coordinated to the nonbridging pyrazole fragment. Cu1 is found in an octahedral coordination environment, ligated equatorially by three N-donors from the side arm of L and an O atom from a water molecule. Axial positions are occupied by the distant N-donor from pyrazole (2.24 Å) and a perchlorate counteranion at an even greater distance (2.761 Å), typical for a Jahn−Teller elongated situation. The second metal is again nested in the dangling chelate arm compartment and is five-coordinate ($\tau = 0.13$) with an additional water in the equatorial position and a perchlorate-O in the axial position. A three-dimensional network is built up by H-bonds between coordinated water molecules, perchlorate anions, and the NH unit of the pyrazole.

Spectroscopic Properties of the Complexes and equilibria in solution. The UV−vis spectra of the complexes **1a**, **2**, and **3** have been recorded in a MeOH/MeCN (5:2) solution, as well as in the solid state (diffuse reflectance).

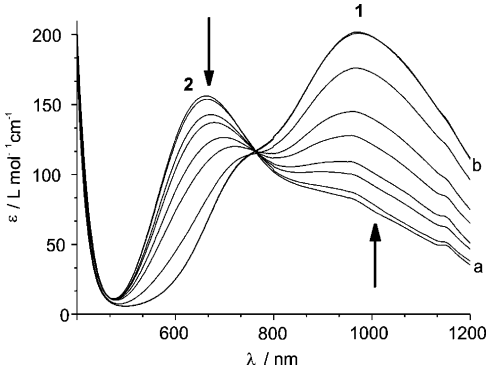

Figure 6. UV−vis titration of a solution of **3** in 0.1 M $NaNO_3$ with NaO*t*Bu between pH 6.55 (a) and 9.40 (b).

Table 3 compares the findings for the ligand field bands for the species in aqueous solution at different pHs, as well as for the isolated compounds. The absorption maxima in the diffuse reflectance spectra are in accordance with the coordination geometries observed crystallographically, that is, trigonal-bipyramidal for **1a** (broad d−d absorption at ∼950 nm), tetragonal for **3** (weak ligand field band at ∼690 nm), and the presence of both signatures in the case of **2**.[22] Similar spectra were observed for each complex in MeOH/MeCN solution, implying that no major structural changes occur upon dissolution of the crystalline solids. The same is true for species in aqueous solution at the respective pH values, except for **2**. In the latter system, the broad d−d absorption at ∼920 nm seen in the diffuse reflectance spectra and in MeOH/MeCN is strongly diminished in aqueous solution around neutral pH. Since a trigonal bipyramidal situation (characterized by the band at ∼920 nm) is observed for the central bis(pyrazolato) bridged dicopper(II) core in **2**, it is reasonable to assume that in aqueous solution the dimeric aggregate largely breaks apart to give bimetallic species $[Cu_2LH_{-1}(H_2O)_x]^{3+}$. It should be noted that pH potentiometry cannot differentiate between bimetallic $[Cu_2LH_{-1}]^{3+}$ and its dimeric aggregate $[(Cu_2LH_{-1})_2]^{6+}$.

Equilibria in solution between the three different complexes could be monitored by UV−vis spectroscopy upon titration with a base, starting at pH 4.66. Dicopper complex **3** was dissolved in 0.1 M $NaNO_3$ (to prevent precipitation of the perchlorate salt **1a** at higher pH), with only $[Cu_2L]^{4+}$ present in solution at pH 4.66. After stepwise addition of base (NaO*t*Bu), the initial dicopper complex was fully converted into $[Cu_2LH_{-1}]^{3+}$ at pH 6.55. Further addition of base led to subsequent formation of $[Cu_2LH_{-2}]^{2+}$ (which is suggested to represent the dinuclear species **1b**, but with a HOH···OH bridge). This becomes the only species at pH 9.4 (Figure 6).

The appropriate amount of base necessary to convert tetranuclear **2** into dicopper(II) complex **1b** was established by titration of complex **2** with base (KO*t*Bu) in MeOH/MeCN (5:2) solution. The concentration of complex **2** was varied in the range from 0.0059 to 0.0027 mol L^{-1}. Titrations were performed by varying the ratio of complex/base from 0.1:1.0 to 2.01:1.0. Complete conversion of tetranuclear **2**

(22) λ_{max} is affected also by the type of donor atoms.

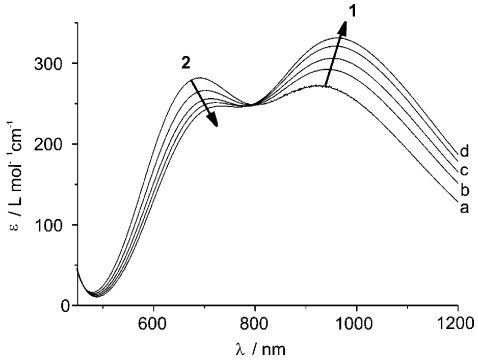

Figure 7. UV−vis spectra of **2** at different concentrations, 0.01 (a), 0.005 (b), 0.003 (c), and 0.002 M (d), in MeOH/MeCN (5:2).

into dinuclear **1b** was observed after the addition of 2 equiv of KO*t*Bu, consistent with the structural data: 2 equiv of base should be required to split the dimeric species into its bimetallic $\{Cu_2L\}$ constituents, concomitant with the formation of the MeOH···OMe bridge.

During the course of these studies, an additional concentration dependence was observed for **2** (Figure 7), suggesting an equilibrium between the tetranuclear complex and a putative dinuclear species **2′** around neutral pH. A concentrated solution of complex **2** (0.01 M in MeOH/MeCN (5:2)) showed two bands at 689 and 923 nm, in accordance with the two types of copper ions found in the solid state (square pyramidal and trigonal bipyramidal). Dilution of this solution causes a shift of the absorption envelope from 923 to 962 and from 689 to 710 nm, with a concomitant increase in intensity for the former and decrease in intensity for the latter band. Spectral features for **2′** are reminiscent of those for **1a**. The equilibrium thus induces a structural reorganization of the copper centers from square pyramidal to trigonal bipyramidal upon dilution, which is likely associated with dissociation of the tetranuclear complex into bimetallic species $[Cu_2LH_{-1}]^{3+}$ (**2′**).

Magnetic Properties. Magnetic susceptibilities for powdered samples of **1a**, **2**, and **3** were measured at two different magnetic fields (2000 and 5000 G) in a temperature range from 2.0 to 295 K. No significant field dependence was observed for any of the complexes. The temperature dependence of the magnetic susceptibility χ_M and of the product $\chi_M T$ for the three distinct systems is depicted in Figure 8.

The observed $\chi_M T$ value for **1a** at 295 K is 0.81 cm^3 K mol^{-1} (2.54 μ_B), which matches the value expected for two uncoupled copper(II) ions (2.54 μ_B for $g = 2.07$). $\chi_M T$ decreases upon lowering of the temperature and reaches zero below 15 K, indicating an $S = 0$ ground state, which is also evident from the broad maximum of the χ_M versus T curve that occurs around 65 K. This is a typical signature for dinuclear copper complexes with relatively strong intramolecular antiferromagnetic coupling. The increase of χ_M at very low temperatures is presumably caused by small amounts (ρ) of paramagnetic impurities.

For complex **2**, the observed $\chi_M T$ value at 295 K is 1.50 cm^3 K mol^{-1} (3.45 μ_B), that is, a bit lower than the value expected for four uncoupled copper(II) ions (3.60 μ_B for $g = 2.08$). $\chi_M T$ gradually decreases with temperature and remains constant (0.84 cm^3Kmol^{-1}, 2.61 μ_B) below 50 K. This behavior can be easily explained on the basis of the structural findings (see below).

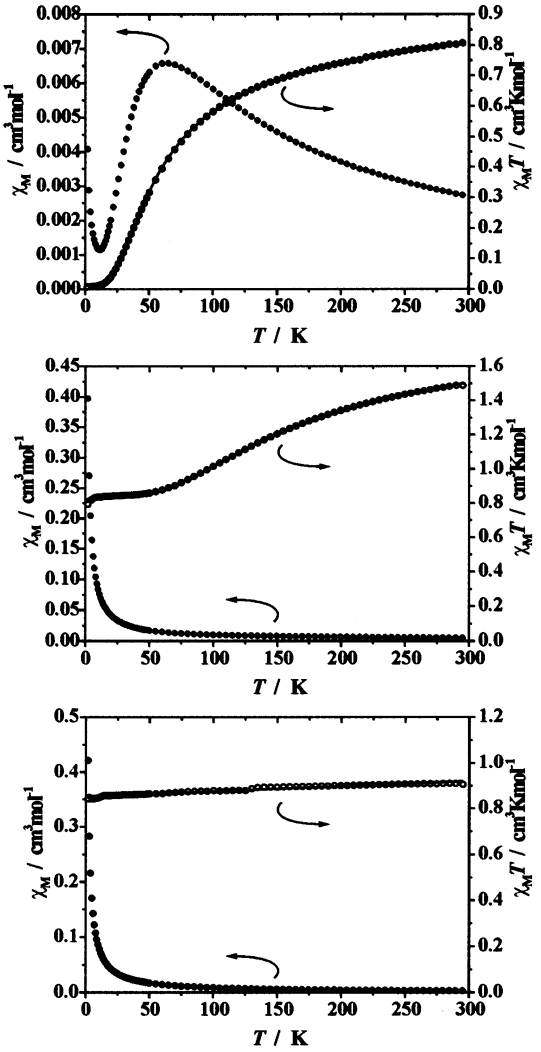

Figure 8. Plots of χ_M (solid circles) and $\chi_M T$ (open circles) versus temperature for **1a** (top), **2** (middle), and **3** (bottom) at 5000 G; the solid lines represent the calculated curve fits (see text).

The observed $\chi_M T$ value at 295 K for dicopper complex **3** is 0.91 cm^3 K mol^{-1} (2.63 μ_B), which indicates the presence of two uncoupled copper(II) ions (2.62 μ_B for $g = 2.14$). In contrast to **1a** and **2**, $\chi_M T$ remains almost constant over a wide temperature range and shows only a slight linear decrease when the temperature is lowered to 2 K, which is a signature for complexes without magnetic interaction.

Experimental data for both dinuclear complexes **1a** and **3** were modeled by using a fitting procedure to the appropriate Heisenberg−Dirac−van Vleck (HDvV) spin Hamiltonian for isotropic exchange coupling and Zeeman splitting, eq 1.[23] A Curie−Weiss-behaved paramagnetic impurity (ρ) with spin $S = 1/2$ and temperature-independent paramagnetism (TIP) were included according to $\chi = (1 - \rho)\chi + \rho\chi_{mono} + TIP$.[24] Susceptibility data for the tetranuclear complex **2** were treated

(23) Kahn, O. *Molecular Magnetism*; Wiley-VCH: New York, 1993.

Table 4. Best Fit Parameters of Magnetic Data Analyses for Complexes **1a**, **2**, and **3**

complex	**1a**	**2**	**3**
g_1	2.07	2.06	2.14
g_2		2.11	
J (cm^{-1})	−35.3	−100.6	0
ρ (%)	2.9	1.9	0.3
TIP ($cm^3\ mol^{-1}$)	3.09×10^{-4}	4.13×10^{-4}	2.27×10^{-4}

in a model that assumes an exchange-coupled bis(μ-pyrazolato)-bridged dicopper(II) core according to eq 1 but with an additional single-ion Curie term for two well-separated non-interacting copper(II) ions (with g_2). Calculated curve fits are shown as solid lines in Figure 8, and best fit parameters for all complexes are summarized in Table 4.

$$H = -2J\vec{S}_1\vec{S}_2 + g\mu_B(\vec{S}_1 + \vec{S}_2)\vec{B} \qquad (1)$$

The differences in the magnetic properties for **1a**, **2**, and **3** can be rationalized on the basis of the crystallographic findings. Tetranuclear **2** has two different types of copper ions: two metal ions constitute the bis(μ-pyrazolato)-bridged core (d(Cu1···Cu1′) = 3.87 Å) and two further ones are coordinated to the remaining ligand side arms and are well separated from the central core (d(Cu1···Cu2′) = 5.52 Å; d(Cu1···Cu2) = 8.32 Å). Antiferromagnetic coupling is observed only within the pyrazolate-bridged core, while the constant value of $\chi_M T$ (0.84 $cm^3\ K\ mol^{-1}$) below 50 K confirms the presence of two additional uncoupled copper(II) ions. Two different g values (2.06 and 2.11) were observed for complex **2**, in agreement with the proposed model. The magnitude of the antiferromagnetic interaction in **1a** containing a single pyrazolate bridge is $-35.3\ cm^{-1}$, which is much lower than for the central part of complex **2** ($-100.6\ cm^{-1}$) with its doubly pyrazolato-bridged dicopper(II) core. It can be safely concluded that the primary pathway for the magnetic interaction is through the pyrazolate bridges, whereas coupling through the H-bonded MeOH···OMe moiety in **1a** should be negligible. The value for the antiferromagnetic interaction in **2**, however, is still relatively small compared to data for various other bis(μ-pyrazolato)-bridged dicopper(II) compounds.[25,26,27] This can be ascribed to the trigonal-bipyramidal coordination geometry imposed by the tripodal tetradentate {N_4} ligand compartments of L and the resulting orientation of the magnetic d_{z^2} orbital of each metal ion, which represents a quite rare situation in copper pyrazolate chemistry.[28] Here the bridging pyrazolate groups in **2** are positioned in such a way that one N atom occupies an axial site on one copper, while the other N atom occupies an equatorial site on the second copper; as a consequence, the overlap of the magnetic d_{z^2} orbitals with ligand orbitals of the metal xy plane is relatively weak. In contrast, many other known dicopper(II) complexes that are spanned by two pyrazolate bridges feature square-planar or tetragonal metal ions where the magnetic $d_{x^2-y^2}$ orbitals are located within the plane of the bridging heterocycles.[25,28] This latter situation establishes a much more efficient coupling pathway and J values on the order of $-200\ cm^{-1}$. It should be noted that additional parameters such as the deviation from coplanarity of the pyrazolate planes,[29] the Cu−N−N angle,[30] the bending angles $\delta_{pz-bend}$ (representing the dihedral angle of the pyrazolate plane relative to the Cu−N−N−Cu plane),[28] and possibly the terminal donor atoms have been found to also contribute to the strength of the antiferromagnetic coupling in bis(pyrazolato)-bridged dicopper(II) scaffolds.

The magnetic behavior of dicopper complex **3**, which does not feature a pyrazolate-bridging motif but which has a large Cu···Cu distance of 6.76 Å, is in accordance with the absence of any efficient exchange pathway and the lack of any significant coupling between the two metal ions. The slight linear decrease of $\chi_M T$ upon lowering of the temperature to 2 K in this case is merely the result of the TIP ($2.27 \times 10^{-4}\ cm^3\ mol^{-1}$).

Conclusions

A new bioinspired pyrazolate-bridging ligand with chelating imidazole-containing side arms has been prepared, and a comprehensive picture of its Cu^{2+} coordination chemistry has been obtained. Different species have been characterized both by potentiometric and crystallographic data depending on the pH or protonation state, respectively, and these species in solution and in the solid state have been correlated through UV−vis spectroscopic investigations. Solid-state structures for **1a**, **1b**, and **2** underline the high tendency of the pyrazole to bridge two metal ions, but only after deprotonation. The species $[Cu_2LH_{-2}]^{2+}$, which is expected to show a rich bioinspired chemistry toward various substrates, predominates above pH 8 in solution and most likely contains a labile HOH···OH or MeOH···OMe bridge, similar to the structure found for **1a** and **1b** in the solid state. The relatively high acidity of the metal-bound water (or methanol) can be explained by the favorable incorporation of the resulting hydroxide (or methoxide) into these strongly H-bonded bridging moieties. Complexes **1**, **2**, and **3** are interconvertible in response to pH changes, which is accompanied by distinct changes in color and magnetic properties. Antiferromagnetic coupling is switched on or off depending on the pyrazole binding mode. The presence of the various species in solution has to be considered when the catalytic activities of this new copper system are probed.

Experimental Section

General. Solvents were purified by established procedures. Bis[2-(1-methylimidazolyl)methyl]amine was prepared from

(24) Simulation of the experimental magnetic data with a full-matrix diagonalization of exchange coupling and Zeeman splitting was performed with the julX program: Bill, E. Max-Planck Institute for Bioinorganic Chemistry, Mülheim/Ruhr, Germany.
(25) (a) Meyer, F.; Jacobi, A.; Zsolnai, L. *Chem. Ber./Recl.* **1997**, *130*, 1441−1447. (b) Teichgräber, J.; Leibeling, G.; Dechert, S.; Meyer, F. *Z. Anorg. Allg. Chem.* **2005**, *631*, 2613−2618.
(26) Bayoñ, J. C.; Esteban, P.; Net, G.; Rasmussen, P. G.; Baker, K. N.; Hahn, C. W.; Gumz, M. M. *Inorg. Chem.* **1991**, *30*, 2572.
(27) Kamiusuki, T.; Okawa, H.; Matsumoto, N.; Kida, S. *J. Chem. Soc., Dalton Trans.* **1990**, 195.
(28) Matsushima, H.; Hamada, H.; Watanabe, K.; Koikawa, M.; Tokii, T. *J. Chem. Soc., Dalton Trans.* **1999**, 971.
(29) Ajò, D.; Bencini, A.; Mani, F. *Inorg. Chem.* **1988**, *27*, 2437.
(30) Hanot, V. P.; Robert, T. D.; Kolnaar, J.; Haasnoot, J. P.; Reedijk, J.; Kooijman, H.; Spek, A. L. *J. Chem. Soc., Dalton Trans.* **1996**, 4275.

1-methyl-1*H*-imidazole according to the literature method,[14] and 3,5-bis(chloromethyl)-1*H*-pyrazole was synthesized in four steps from 3,5-dimethyl-1*H*-pyrazole.[4] All other chemicals were purchased from commercial sources and were used as received. Microanalyses were performed by the Analytisches Labor des Anorganisch-Chemischen Instituts der Universität Göttingen. IR spectra (as KBr pellets) were recorded with a Digilab Excalibur, and UV−vis spectra of solutions and solids (diffuse reflectance) were recorded with a Varian Cary 5000 spectrometer at room temperature. The mass spectra were measured with a Finnigan MAT 95 (FAB-MS) or a Finnigan MAT 8200 (ESI-MS), and the NMR spectra were recorded with a Bruker Avance 200 at room temperature (^{1}H, 200.13 MHz; ^{13}C, 50.3 MHz). The residual solvent signal was used as the chemical shift reference ($CDCl_3$, $\delta_H = 7.24$, $\delta_C = 77.0$). Magnetic data were measured with a Quantum-Design MPMS-5S SQUID magnetometer equipped with a 5 T magnet in the range from 295 to 2 K. The powdered samples were contained in a gel bucket and fixed in a nonmagnetic sample holder.

Caution! Although no problems were encountered in this work, transition metal perchlorate complexes are potentially explosive and should be handled with proper precautions.

Synthesis of 3,5- Bis{bis[2-(1-methylimidazolyl)methyl]-aminomethyl}pyrazole (L). Bis[2-(1-methylimidazolyl)methyl]-amine (20.50 g, 0.10 mol) and 3,5-bis(chloromethyl)-1*H*-pyrazole (8.25 g, 0.05 mol) were dissolved in 700 mL of acetonitrile, and Na_2CO_3 (53 g, 0.50 mol, predried at 100−120 °C and 10^{-3} mbar) was added to this solution. The reaction mixture was refluxed for 24 h. After filtration, the solvent was evaporated, and the residue was dried at 60 °C and 10^{-3} mbar for 12 h. L was obtained as a light yellow solid (20.80 g, 83%). mp: 78−80 °C. MS (EI): *m*/*z* (%) 502 (5), [M^+], 407 (100), [M^+ − 2-methylene-*N*-methylimidazole]. ^{1}H NMR ($CDCl_3$): δ 3.45 (s, CH_3, 12H), 3.57 (s, pzCH_2, 4H), 3.62 (s, NCH_2, 8H), 6.14 (s, pz-H^4, 1H), 6.79 (d, $J = 1$ Hz, im-CH, 4H), 6.91 (d, $J = 1$ Hz, im-CH, 4H). ^{13}C NMR ($CDCl_3$): δ 32.4 (CH_3), 49.0 (CH_2), 48.6 (CH_2), 106.7 (pz-C^4), 121.4 (im-C), 127.0 (im-C), 145.0 (im-C^2); pz-C$^{3/5}$ not observed. Anal. Calcd (%) for $C_{25}H_{34}N_{12}\cdot H_2O$ (520.6 g mol^{-1}): C, 57.67; H, 6.58; N, 32.28. Found: C, 57.88; H, 6.81; N, 32.78.

Preparation of $[Cu_2LH_{-1}(OMe)(MeOH)](ClO_4)_2$ (1a). A solution of L (2.63 g, 5.24 mmol) in methanol (100 mL) was treated with KO^{t}Bu (0.58 g, 5.24 mmol) and stirred for 10 min at room temperature. $Cu(NO_3)_2\cdot 3H_2O$ (2.51 g, 10.48 mmol) was then added, and stirring of the green mixture was continued for 2 h. After the addition of H_2O (900 mL), the mixture was purified by ion-exchange chromatography on a SP-Sephadex C25 column. The main blue fraction was collected by washing the column with a 0.4 M solution of $NaNO_3$. The solvent was evaporated, and the residue was extracted three times with MeCN to remove $NaNO_3$. The combined MeCN phases were evaporated to dryness, and the residue was redissolved in water. A 0.2 M NaOH solution was then slowly added until the solution reached pH 9, concomitant with a color change from blue to deep green. The addition of excess $NaClO_4$ yielded a green precipitate, which was separated by filtration and dried. Slow diffusion of Et_2O into a solution of the crude product in CH_3CN/CH_3OH (2:1) led to the formation of green crystals of **1a**·MeCN (2.92 g, 60%). IR (KBr, cm^{-1}): ν 3458 (s), 3132 (w), 1555 (m), 1509 (w), 1454 (w), 1381 (w), 1286 (w), 1086 (vs), 953 (w), 871 (w), 665 (w), 626 (m). MS (FAB, glycerin): *m*/*z* (%) 726 (10) [$Cu_2LH_{-1}(ClO_4)^+$], 627 (100) [$Cu_2LH_{-1}^+$]. Anal. Calcd (%) for $C_{27}H_{40}Cu_2N_{12}Cl_2O_{10}\cdot$MeCN (931.7 g mol^{-1}): C, 34.80; H, 4.29; N, 18.04. Found: C, 34.82; H, 4.27; N, 18.96.

Preparation of $[Cu_2LH_{-1}(OMe)(MeOH)](NO_3)_2$ (1b). A solution of L (0.10 g, 0.20 mmol) in 50 mL of methanol was treated with 2 equiv of KO*t*Bu (0.04 g, 0.40 mmol), and the solution was stirred for 10 min. $Cu(NO_3)_2\cdot 3H_2O$ (0.09 g, 0.40 mmol) was then added, and stirring of the resulting green mixture was continued for 2 h at room temperature. After evaporation of all volatile material, the remaining green solid was redissolved in a mixture of CH_3CN/CH_3OH (2:1). Slow diffusion of Et_2O into this solution led to the formation of green crystals of **1b**·2MeOH. IR (KBr, cm^{-1}): ν 3429 (s), 2943 (w), 1508 (m), 1355 (vs), 1283 (w), 1160 (w), 1095 (w), 1036 (w), 951 (w), 874 (w), 759 (w). MS (FAB, glycerin): *m*/*z* (%) 689 (10) [$Cu_2LH_{-1}(NO_3)^+$], 627 (100) [$Cu_2LH_{-1}^+$]. Anal. Calcd (%) for $C_{27}H_{40}Cu_2N_{14}O_8\cdot$2MeOH (879.9 g mol^{-1}): C, 39.59; H, 5.50; N, 22.29. Found: C, 39.76; H, 5.35; N, 22.73.

Preparation of $[Cu_2LH_{-1}(NO_3)(H_2O)]_2(NO_3)_4$ (2). A solution of L (2.63 g, 5.24 mmol) in methanol (100 mL) was treated with KO^{t}Bu (0.58 g, 5.24 mmol) and was stirred for 10 min at room temperature. $Cu(NO_3)_2\cdot 3H_2O$ (2.51 g, 10.48 mmol) was then added, and stirring of the green mixture was continued for 2 h. After the addition of H_2O (900 mL), the mixture was purified by ion-exchange chromatography on a SP-Sephadex C25 column. The main blue fraction was collected by washing the column with a 0.4 M solution of $NaNO_3$. From this aqueous solution, green-blue crystals of **2**·5H_2O were obtained (3.44 g, 75%). IR (KBr, cm^{-1}): ν 3420 (m), 3125 (w), 1624 (w), 1509 (m), 1352 (vs), 1167 (w), 1093 (w), 1011 (w), 951 (w), 872 (w), 831 (w), 754 (m). MS (FAB, 3-NBA): *m*/*z* (%) 689 (50) [$Cu_2LH_{-1}(NO_3)^+$], 627 (100) [$Cu_2LH_{-1}^+$]. Anal. Calcd (%) for $C_{50}H_{80}Cu_4N_{30}O_{25}\cdot 5H_2O$ (1755.60 g mol^{-1}): C, 34.21; H, 4.59; N, 23.94. Found: C, 34.76; H, 4.50; N, 23.73.

Preparation of $[Cu_2L(H_2O)_2(ClO_4)](ClO_4)_3$ (3). Aqueous $HClO_4$ (5−10%) was slowly added to a solution of **2** (0.17 g, 0.10 mmol) in 10 mL of water until pH 4 was reached. After the addition of 5 mL of methanol (or ethanol), the solution was left standing for 2 days, during which time slow evaporation of the solvent led to the formation of blue crystals of **3**·2H_2O (0.18 g, 86%). IR (KBr): ν 3460 (w), 1628 (w), 1555 (w), 1509 (w), 1381 (w), 1088 (vs), 626 (m), cm^{-1}. MS (FAB, 3-NBA): *m*/*z* (%) 825 (50) [$Cu_2LH_{-1}(ClO_4)_2^+$], 726 (55) [$Cu_2LH_{-1}(ClO_4)^+$], 627 (75) [$Cu_2LH_{-1}^+$]. Anal. calcd (%) for $C_{25}H_{38}Cl_4Cu_2N_{12}O_{18}\cdot 2H_2O$ (1099.6 g mol^{-1}): C, 27.28; H, 3.82; N, 15.27. Found: 27.77; H, 3.96; N, 15.23.

pH Potentiometric Titrations. The pH potentiometric titrations were conducted at 25.0 ± 0.1 °C at an ionic strength of 0.2 M (KCl) using a Radiometer PHM 84 pH meter equipped with a Metrohm 6.0234.100 combined electrode and a Metrohm dosimat 715. Calibration of the electrode and pH meter was performed using a buffer of potassium biphtalate at pH 4.008. Concentrations of the stock solutions (HCl 0.2004 M and KOH 0.1972 M) were checked, and a pK_W of 13.784 and an Irving factor of 0.079 were obtained following Gran's method.[31] Concentrations of the ligand stock solutions were also determined by Gran's method. The metal ion stock solution was prepared from $CuCl_2\cdot 2H_2O$ (Reanal) dissolved in doubly distilled water. The concentration of the metal ion stock solution was determined gravimetrically via precipitation with quinolin-8-olate.

pH-metric titrations were performed in the pH range of 2.0−10.5 or until precipitation, on samples of 4.00 mL, at an ionic strength of 0.2 M (KCl), and at 25 ± 0.1 °C. Purified, strictly oxygen-free argon was continuously bubbled through the samples

(31) Gran, G. *Analyst* **1952**, *77*, 661−671.

Table 5. Crystal Data and Refinement Details for **1a**, **1b**, **2**, and **3**

	1a	**1b**	**2**	**3**
formula	$C_{27}H_{40}Cu_2N_{12}O_2^{2+}$, $2ClO_4^-$, C_2H_3N	$C_{27}H_{40}Cu_2N_{12}O_2^{2+}$, $2NO_3^-$, $2CH_4O$	$C_{50}H_{70}Cu_4N_{26}O_8^{4+}$, $4NO_3^-$, $5H_2O$	$C_{25}H_{38}Cl_1Cu_2N_{12}O_6^{3+}$, $3ClO_4^-$, $2H_2O$
M_r	931.74	879.89	1755.60	1099.59
cryst size (mm)	0.46 × 0.24 × 0.21	0.40 × 0.23 × 0.12	0.50 × 0.26 × 0.21	0.50 × 0.08 × 0.07
cryst syst	monoclinic	Triclinic	triclinic	orthorhombic
space group	*Cc* (No. 9)	$P\bar{1}$ (No. 2)	$P\bar{1}$ (No. 2)	*Pbca* (No. 61)
a (Å)	18.1991(9)	11.1984(4)	9.5728(6)	18.1999(8))
b (Å)	16.9395(6)	14.9118(6)	13.1348(8)	17.0313(5)
c (Å)	13.6063(8)	24.3582(9)	14.5660(9)	26.7503(9)
α (deg)	90	101.663(3)	94.003(5)	90
β (deg)	112.350(4)	99.134(3)	106.635(5)	90
γ (deg)	90	100.299(3)	93.850(5)	90
V (Å^3)	3879.5(3)	3838.4(3)	1743.26(19)	8291.7(5)
Z	4	4	1	8
ρ_{calcd} [g cm^{-3}]	1.595	1.523	1.672	1.762
F(000)	1920	1832	906	4496
μ (mm^{-1})	1.305	1.180	1.305	1.377
T_{max}/T_{min}	0.7515/0.5886	0.8059/0.5238	0.7711/0.5865	0.9343/0.7870
hkl range	±21, ±19, −16−15	±13, −15−17, ±28	±11, ±15, −15−17	±21, −17−20, −31−27
θ range (deg)	1.71−24.81	1.43−24.79	1.56−24.74	1.81−24.89
measured reflns	29 113	57 759	27 830	78 080
unique reflns [R_{int}]	6527 [0.0651]	13 096 [0.0591]	5954 [0.0554]	7173 [0.1116]
obsd reflns ($I > 2\sigma(I)$)	6123	9972	5232	4914
ref params/restraints	553/4	1010/36	563/38	627/58
GOF	1.001	1.017	1.040	1.005
R1, wR2 ($I>2\sigma(I)$)	0.0287, 0.0674	0.0520, 0.1262	0.0312, 0.0836	0.0481, 0.1100
R1, wR2 (all data)	0.0314, 0.0682	0.0743, 0.1367	0.0364, 0.0860	0.0806, 0.1211
residual electron density (e Å^{-3})	0.351/−0.275	1.439/−0.743	0.439/−0.533	0.828/−0.490

during the titrations. The ligand concentrations were varied in the range of $1 \times 10^{-3}-2 \times 10^{-3}$ M and the metal to ligand ratios were 1:1, 1.5:1, and 2:1.

The pH-metric results were utilized to establish the stoichiometry of species and to calculate the stability constants. Calculations were performed with the computer programs SUPERQUAD and PSEQUAD,[32] while the speciation curves were created with the help of the MEDUSA program.[33]

X-ray Crystallography. X-ray data were collected on a STOE IPDS II diffractometer (graphite-monochromated Mo Kα radiation, $\lambda = 0.71073$ Å) by use of ω scans at −140 °C (Table 5). The structures were solved by direct methods and refined on F^2 using all reflections with SHELX-97.[34] Most of the non-hydrogen atoms were refined anisotropically. Unless otherwise noted, hydrogen atoms were placed in calculated positions and assigned to an isotropic displacement parameter of 0.08 Å^2.

Three oxygen atoms of one ClO_4^- anion and the O2-bound methyl group in **1a** are disordered about two positions (occupancy factors of 0.563(12)/0.437(12) and 0.73(4)/0.27(4)). A DFIX restraint ($d_{O-C} = 1.41$ Å) was applied to model the disorder of the methanol. The positional and isotropic displacement parameters of the hydrogen atom H1 were refined without any restraints or constraints. The absolute structure parameter of **1a** ($x = -0.001(8)$) was determined according to Flack with SHELX-97.[35] Three methanol solvent molecules and three oxygen atoms of one NO_3^- anion in **1b** are disordered about two positions (occupancy factors of 0.844(9)/0.156(9), 0.683(10)/0.317(10), 0.775(8)/0.225(8), and 0.709(12)/0.291(12)). DFIX ($d_{O-C} = 1.41$ Å) and SADI restraints (d_{N-O}, $d_{O\cdots O}$) were used to model the disorder. The atoms of the disordered parts were refined isotropically. The positions of the hydrogen atoms H1A and H1B were refined without restraints. A fixed isotropic displacement parameter of 0.08 Å^2 was assigned to those hydrogen atoms. One NO_3^- anion in **2** was found to be disordered about two positions (occupancy factors of 0.672(8)/0.328(8)), and SADI restraints (d_{N-O}, $d_{O\cdots O}$) were used to model the disorder. Additionally, a water molecule is disordered about a center of inversion and was refined with a fixed occupancy factor of 0.5. The positions of the hydrogen atoms bound to the oxygen atoms O11, O12, and O13 of the respective water molecules were refined using DFIX restraints ($d_{O-H} = 0.83$ Å, $d_{H\cdots H}$ (H11A/B, H13A/B) = 1.3 Å). A fixed isotropic displacement parameter of 0.08 Å^2 was assigned to those hydrogen atoms. The positional and isotropic displacement parameters of the hydrogen atoms H1A and H1B of the copper-bound water molecule were refined without any restraints or constraints. The oxygen atoms of one ClO_4^- anion and one water molecule in **3** are disordered about two positions (occupancy factors of 0.785(4)/0.215(4) and 0.63(4)/0.37(4)). SADI restraints (d_{Cl-O}, $d_{O\cdots O}$) and EADP constraints were used to model the disorder of the ClO_4^-. The positions of the hydrogen atoms of all water molecules and the N−H hydrogen were refined using DFIX restraints ($d_{O-H} = 0.83$ Å, $d_{N-H} = 0.93$ Å, and $d_{H\cdots H} = 1.3$ Å). A fixed isotropic displacement parameter of 0.08 Å^2 was

(32) (a) Gans, P.; Sabatini, A.; Vacca, A. *J. Chem. Soc., Dalton Trans.* **1985**, 1195−1200; (b) Zékány, L.; Nagypál, I. In *Computational Methods for the Determination of Stability Constants*; Leggett, D.L., Ed.; Plenum Press: New York, 1985; pp 291−353.

(33) Puigdomenech, I. *MEDUSA and Hydra software for chemical equilibrium calculations*; Royal Institute of Technology (KTH): Stockholm, Sweden.

(34) (a) Sheldrick, G. M. *SHELXL-97, Program for Crystal Structure Refinement*; University of Göttingen: Göttingen, Germany, 1997. (b) Sheldrick, G. M. *SHELXS-97, Program for Crystal Structure Solution*; University of Göttingen: Göttingen, Germany, 1997.

(35) Flack, H. D. *Acta Crystallogr.* **1983**, *A39*, 876−881.

assigned to the hydrogen atoms bound to O3 and O4A/B. Face-indexed absorption corrections were performed numerically with the program X-RED.[36]

Acknowledgment. A.P. is grateful to the Gottlieb Daimler- and Karl Benz-foundation for a PhD fellowship. This work was supported by the Deutsche Forschungsgemeinschaft (DFG Me1313/7-1) and the Hungarian Scientific Research Fund (OTKA T049612).

Supporting Information Available: Crystallographic data, in CIF format for **1a**, **1b**, **2**, and **3**, ORTEP plot of **1b** (Figure S1), titration curve of L (Figure S2), and titration curve of L with 2 equiv Cu^{2+} (Figure S3). This material is available free of charge via the Internet at http://pubs.acs.org.

IC062434M

(36) *X-RED*; STOE & CIE GmbH: Darmstadt, Germany, 2002.